

Topology of $\text{Ge}_x\text{Se}_{1-x}$ ($0 \leq x \leq 0.4$) glasses

I. Petri & P. S. Salmon¹

Department of Physics, University of Bath, Bath BA2 7AY, UK

The topology of bulk quenched $\text{Ge}_x\text{Se}_{1-x}$ glasses at compositions $x=0, 0.2, 0.25, 0.33$ and 0.4 was studied by using neutron diffraction to measure the Bhatia–Thornton number–number partial structure factor, $S_{\text{NN}}(Q)$, where Q is the scattering vector. The results were analysed by reference to the recently measured full set of partial pair distribution functions for glassy GeSe_2 which help to illustrate the origin of the main structural features and give insights into the chemical ordering. Addition of Ge to glassy Se imposes an additional length scale on the atomic ordering, associated with intermediate ranged Ge–Ge correlations, which is manifested by a so called first sharp diffraction peak at $Q_{\text{FSDP}} \approx 1 \text{ \AA}^{-1}$ that reaches its maximum height at the GeSe_2 composition. The results are consistent with the ‘8-N’ rule and may be interpreted in terms of a chemically ordered continuous random network. However, the full set of partial pair distribution functions measured for glassy GeSe_2 show that deviations from this model do occur and may, therefore, be expected for other glasses near this composition.

The object of this paper is to study the change in topology of bulk quenched $\text{Ge}_x\text{Se}_{1-x}$ glasses over a wide composition range by using neutron diffraction to measure the Bhatia–Thornton⁽¹⁾ number–number partial structure factor, $S_{\text{NN}}(Q)$, where Q is the magnitude of the scattering vector. The Ge–Se system was chosen for investigation since it is a much studied covalently bonded glass former whose network connectivity over the glass forming region $0 \leq x \leq 0.43$ ⁽²⁾ can be changed by altering the Ge:Se ratio. On the basis of mean field constraint theory, there is a rigidity percolation threshold at $x=0.2$ corresponding to a mean coordination number $\bar{n}=2.4$. Evidence for such a transition and related phenomena near this \bar{n} value has been found from Raman spectroscopy and temperature modulated differential scanning calorimetry measurements.^(3–5) The present work complements other neutron diffraction experiments on the composition and temperature dependence of the structure of both the liquid^(6–8) and glassy⁽⁹⁾ phases of $\text{Ge}_x\text{Se}_{1-x}$. Other studies on the composition dependence of the glass structure have been made using both direct and indirect methods, including x-ray^(10,11) and electron^(12,13) diffraction, extended x-

ray absorption fine structure (EXAFS),^(14,15) x-ray emission⁽¹⁶⁾ and Raman^(3,5,17,18) spectroscopy. Unexpected deviations from the ‘8-N’ rule⁽¹⁹⁾ were observed in some of this work.^(11,15) In the present investigation, the diffraction patterns for the glassy phase were measured over an extended Q range which will reduce the distortion of the corresponding real space functions. Furthermore, advantage is taken of the recently measured full set of partial pair distribution functions, $g_{\alpha\beta}(r)$, for glassy GeSe_2 ⁽²⁰⁾ in the interpretation of the results.

The total structure factor $S_{\text{T}}(Q)$ measured in a neutron diffraction experiment on a binary system comprising Ge and Se of natural isotopic abundance reduces, at a good level of approximation, to the single partial structure factor $S_{\text{NN}}(Q)$ since the coherent scattering lengths of Ge and Se are similar.^(6,8) The Fourier transform of this function, $g_{\text{NN}}(r)$, contains information on the topology of the system as it describes the sites of the scattering nuclei but is not concerned with their chemical identity. For many binary glasses and their corresponding liquids, $S_{\text{NN}}(Q)$ has a characteristic three peak structure for $0 \leq Qr_1 \leq 10$, where r_1 is the nearest neighbour distance, which is manifest in the corresponding $S_{\text{T}}(Q)$.^(21,22) The first of these peaks, occurring at low values of Qr_1 between ≈ 2.1 and ≈ 3.1 for many oxide, halide and chalcogenide structurally disordered systems,⁽²³⁾ is the so-called first sharp diffraction peak (FSDP). It is a signature that the bonding takes a significant directional character and arises from the intermediate ranged atomic ordering.^(22–4) The present experiments on glassy $\text{Ge}_x\text{Se}_{1-x}$ will, therefore, provide information on the network topology at both short and intermediate atomic length scales.

Theory

In a neutron diffraction study of a binary Ge–Se compound, the coherent scattered intensity can be represented by the total structure factor

$$S_{\text{T}}(Q) = [S_{\text{NN}}(Q) - 1] + A\{[S_{\text{CC}}(Q)/x(1-x)] - 1\} + BS_{\text{NC}}(Q) \quad (1)$$

where x denotes the atomic fraction of Ge, b_{α} the coherent scattering length of chemical species α , $\Delta b = b_{\text{Ge}} - b_{\text{Se}}$, $\langle b \rangle = \{xb_{\text{Ge}} + (1-x)b_{\text{Se}}\}$, $A = x(1-x)\Delta b^2 / \langle b \rangle^2$ and $B = 2\Delta b / \langle b \rangle$. In Equation (1) $S_{\text{NN}}(Q)$, $S_{\text{CC}}(Q)$ and $S_{\text{NC}}(Q)$ are the Bhatia–Thornton⁽¹⁾ number–number, concentration–concentration and number–concentration

¹ Author to whom correspondence should be addressed. (e-mail: p.s.salmon@bath.ac.uk)

tion partial structure factors respectively. The total pair distribution function follows from the Fourier transform relation

$$G_T(r) = \frac{1}{2\pi^2 n_0 r} \int_0^\infty dQ S_T(Q) Q \sin(Qr) = [g_{\text{NN}}(r) - 1] + A g_{\text{CC}}(r) + x(1-x) B g_{\text{NC}}(r) \quad (2)$$

where n_0 is the atomic number density. In terms of the partial pair distribution functions for the Ge and Se atomic species

$$g_{\text{NN}}(r) = x^2 g_{\text{GeGe}}(r) + (1-x)^2 g_{\text{SeSe}}(r) + 2x(1-x) g_{\text{GeSe}}(r) \quad (3a)$$

$$g_{\text{CC}}(r) = x(1-x) [g_{\text{GeGe}}(r) + g_{\text{SeSe}}(r) - 2g_{\text{GeSe}}(r)] \quad (3b)$$

$$g_{\text{NC}}(r) = x g_{\text{GeGe}}(r) - (1-x) g_{\text{SeSe}}(r) + (1-2x) g_{\text{GeSe}}(r) \quad (3c)$$

whence it follows that

$$G_T(r) = C [g_{\text{GeSe}}(r) - 1] + D [g_{\text{SeSe}}(r) - 1] + E [g_{\text{GeGe}}(r) - 1] \quad (4)$$

where $C = 2x(1-x) b_{\text{Ge}} b_{\text{Se}} / \langle b \rangle^2$, $D = (1-x)^2 b_{\text{Se}}^2 / \langle b \rangle^2$ and $E = x^2 b_{\text{Ge}}^2 / \langle b \rangle^2$. If the scattering lengths of the atomic species are equal then $\Delta b = 0$ and the functions $S_{\text{NN}}(Q)$ and $g_{\text{NN}}(r)$ are given directly by Equations (1) and (2). Since $x \bar{n}_{\text{Ge}}^{\text{Ge}} = (1-x) \bar{n}_{\text{Se}}^{\text{Se}}$ it follows from the definition of $g_{\text{NN}}(r)$ that the average coordination number, irrespective of species type, is given by

$$\bar{n} = 4\pi n_0 \int_{r_i}^{r_j} r^2 g_{\text{NN}}(r) dr = x (\bar{n}_{\text{Ge}}^{\text{Ge}} + \bar{n}_{\text{Ge}}^{\text{Se}}) + (1-x) (\bar{n}_{\text{Se}}^{\text{Se}} + \bar{n}_{\text{Se}}^{\text{Ge}}) \quad (5)$$

where \bar{n}_α^β is the mean number of particles of type β contained in a volume defined by two concentric spheres of radii r_i and r_j , centred on a particle of type α . For a binary Ge-Se system comprising elements of natural isotopic abundance the neutron scattering lengths are comparable at $b_{\text{Ge}} = 8.185(20)$ fm and $b_{\text{Se}} = 7.970(9)$ fm.⁽²⁵⁾ The weighting coefficients for the investigated glasses are given in Table 1 and show that $S_{\text{NN}}(Q)$ accounts for the majority of $S_T(Q)$, i.e. the contribution from the other partial structure factors can, to first order, be neglected.

In practice, the reciprocal space data sets are limited by the measurement window function $M(Q)$ of the diffractometer where $M(Q \leq Q_{\text{max}}) = 1$ and $M(Q > Q_{\text{max}}) = 0$ and it is convenient to consider the function

$$D'(r) = \frac{2}{\pi} \int_0^\infty dQ S_T(Q) M(Q) Q \sin(Qr) = 4\pi r n_0 G_T(r) \otimes M(r) \quad (6)$$

where \otimes denotes the one dimensional convolution operator and $M(r)$ is the real-space representation of $M(Q)$. Since $G_T(r)$ is dominated by $g_{\text{NN}}(r)$ and $M(Q=0) = 1$ it then follows that

$$D'(r) \approx [4\pi r n_0 g_{\text{NN}}(r) \otimes M(r)] - 4\pi r n_0 \quad (7)$$

To obtain reliable coordination numbers for the glasses it proved necessary to take into explicit account the effect of the finite Q_{max} . The first peak of $D'(r)$ was therefore fitted to a sum of Gaussians representing the individual $t_{\alpha\beta}(r) \equiv 4\pi r n_0 g_{\alpha\beta}(r)$, convoluted with $M(r)$.

Experimental method

Glassy $\text{Ge}_x\text{Se}_{1-x}$ samples were prepared by loading Ge lumps (99.9999%, Aldrich) and Se pellets (99.999%, Johnson Matthey) into silica ampoules of 5 mm internal diameter and 1 mm wall thickness in a high purity argon filled glove box (≈ 1 ppm oxygen, < 10 ppm water). The ampoules had been cleaned using chromic acid prior to etching with a 40% solution of hydrofluoric acid. The sample filled ampoules were then evacuated to a pressure of $\approx 10^{-5}$ torr, purged three times with helium gas and after ≈ 12 h they were sealed. Next, the ampoules were loaded into a rocking furnace and were heated at 1°C min^{-1} to 1000°C pausing for 1 h at both the melting and boiling points of Se and at the melting point of Ge. After 48 h the ampoules were slowly cooled to either 850°C ($x=0.33$), 750°C ($x=0.25$ or 0.4) or 650°C ($x=0.2$) where they were equilibrated for ≈ 4 h and quenched in an ice/salt water mixture at -5°C . Glassy Se was prepared by heating the ampoule at 1°C min^{-1} to 210°C , near the melting point of Se, where it was equilibrated for 3 h. It was then heated at the same rate to 450°C , left for ≈ 12 h and finally quenched in an ice/salt water mixture at -5°C . The glass transition temperature, T_g , of the samples was measured using a TA Instruments Thermal Analyst 2000 machine operating at a scan rate of $10^\circ\text{C min}^{-1}$. Both the onset and midpoint temperatures of the transition were recorded (Table 1) and lie within the range of values given in the literature for $\text{Ge}_x\text{Se}_{1-x}$ glasses.^(2,3,5,26-9)

The neutron diffraction experiment on the $x=0.2$ sample was performed using the D4B instrument at the Institut Laue-Langevin (Grenoble, France) operating at an incident wavelength of 0.7047 \AA . The remaining experiments were made using the SANDALS instrument at the ISIS pulsed neutron source (Rutherford Appleton Laboratory, UK). The glasses were in the form of a coarsely ground powder and were contained in cylindrical vanadium cans of outer diameter 7 mm ($x=0.2$ and 0.33) or 9 mm (all other x) and wall thickness 0.1 mm at a temperature of $26(1)^\circ\text{C}$. Each complete diffraction experiment comprised measure-

Table 1. Weighting factors for the partial pair correlation functions, glass transition temperature and number density for $\text{Ge}_x\text{Se}_{1-x}$ glasses

Glass	x	A	B	C	D	E	$T_g(\text{onset})$ ($^\circ\text{C}$)	$T_g(\text{midpoint})$ ($^\circ\text{C}$)	n_0 (\AA^{-3})
Se	0	-	-	-	1	-	51(2)	53(2)	0.0327 ⁽²⁶⁾
GeSe_4	0.2	1.15×10^{-4}	0.0537	0.3251	0.6331	0.0417	167(4)	191(3)	0.0339 ⁽²⁶⁾
GeSe_3	0.25	1.35×10^{-4}	0.0536	0.3800	0.5550	0.0650	231(4)	253(3)	0.0339 ⁽²⁶⁾
GeSe_2	0.33	1.59×10^{-4}	0.0535	0.4483	0.4366	0.1151	396(3)	415(3)	0.0334 ⁽²⁾
$\text{GeSe}_{1.5}$	0.4	1.71×10^{-4}	0.0534	0.4825	0.3524	0.1652	341(3)	351(3)	0.0341 ⁽²⁶⁾

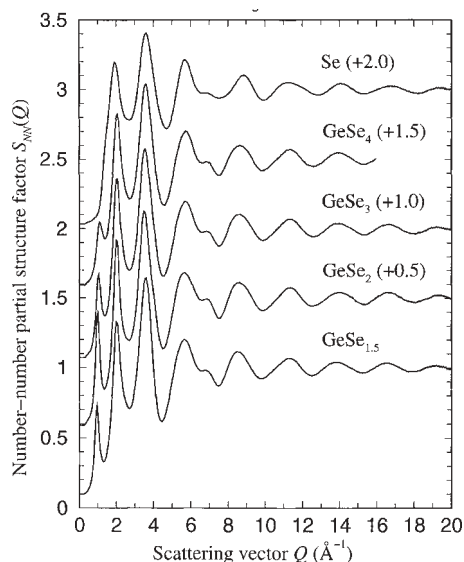


Figure 1. Bhatia–Thornton number–number partial structure factor $S_{NN}(Q)$ for $\text{Ge}_x\text{Se}_{1-x}$ glasses as obtained from Equation (1) by assuming $A=B=0$. The vertical bars give the statistical errors on the data points and are comparable to the line thickness

ment of the diffraction patterns for the samples in their container, the empty container, nothing placed at the sample position and a vanadium rod of diameter comparable to the sample for normalisation purposes. In the D4B experiment, the diffraction pattern for a cadmium rod of diameter equal to the sample was also measured to account for the effect of sample self shielding on the background count rate at small scattering angles.⁽³⁰⁾ The SANDALS data analysis was made using the ATLAS suite of programs⁽³¹⁾ while the D4B data analysis followed the scheme outlined elsewhere.⁽³²⁾ The nuclear cross sections required for the data processing were taken from Sears.⁽²⁵⁾

The final $S_T(Q)$ functions were constructed by merging all those diffraction patterns from the different detector groups of an instrument that showed good agreement. It was checked that the resultant $S_T(Q)$ functions tend to the correct high Q limit, obey the usual sum rule relation and that there is good overall agreement between each $S_T(Q)$ and the back Fourier transform of the corresponding $G_T(r)$ after the unphysical low r oscillations are set to their calculated limiting $G_T(0)$ value.⁽³³⁾

Results

The measured $S_{NN}(Q)$, as obtained from Equation (1) by assuming $A=B=0$, are shown in Figure 1. As x is increased from zero, the most striking change is the appearance of an FSDP at a position $Q_{\text{FSDP}} \approx 1 \text{ \AA}^{-1}$ (see Table 2), i.e. a new intermediate ranged atomic length scale of periodicity $2\pi/Q_{\text{FSDP}}$ develops as Ge is added

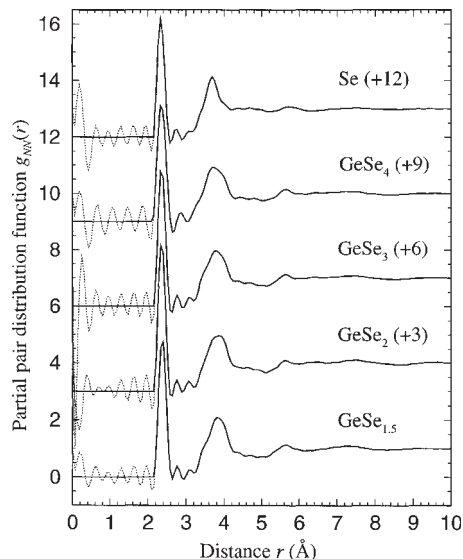


Figure 2. Bhatia–Thornton number–number partial pair distribution function $g_{NN}(r)$ for $\text{Ge}_x\text{Se}_{1-x}$ glasses as obtained from Equation (2) by assuming $A=B=0$. The extent of the low r oscillations about $g_{NN}(0)=0$, that arise from the Fourier transform procedure, are shown by the broken curves

to pure Se.⁽²⁴⁾ The extent of these oscillations in real space is controlled by the coherence length $2\pi/\Delta Q_{\text{FSDP}}$ where ΔQ_{FSDP} , the full width at half maximum of the FSDP, was obtained by reflecting the low Q part of the peak about Q_{FSDP} . The magnitude of the oscillations is controlled by the height of the FSDP which first increases with x , reaching its maximum at GeSe_2 , before subsequently decreasing. The resolution function, $\Delta Q/Q$, of the D4B and SANDALS instruments in the region of the FSDP are roughly comparable at $\approx 2\%$. The $g_{NN}(r)$ functions for the $\text{Ge}_x\text{Se}_{1-x}$ glasses are shown in Figure 2 and were obtained from Equation (2) by assuming $A=B=0$ and using reciprocal space data sets truncated at a maximum value Q_{max} of either 15.95 \AA^{-1} ($x=0.2$) or 19.95 \AA^{-1} (all other x). The peak positions and coordination numbers are summarised in Table 3. Simple integration of the first peak in $g_{NN}(r)$ from its first to second minimum gave \bar{n} values that were too high compared with those expected on the basis of the ‘8-N’ rule⁽¹⁹⁾ and the measured $g_{\alpha\beta}(r)$ for GeSe_2 .⁽²⁰⁾ The \bar{n} values of Table 3 were, therefore, obtained by taking into *explicit* account the finite measurement window function of the diffractometer through the peak fitting procedure described in the Theory section.

Discussion

The $g_{NN}(r)$ for glassy Se shows that each Se atom is bound to two other Se, in accordance with the ‘8-N’ rule, at a distance of $2.34(2) \text{ \AA}$. The glass structure is

Table 2. Parameters describing $S_{NN}(Q)$ for glassy $\text{Ge}_x\text{Se}_{1-x}$ where Q_ϵ ($\epsilon = \text{FSDP}, 2, 3$ or 4) denotes peak position

Glass	Q_{FSDP} (\AA^{-1})	Height of FSDP	ΔQ_{FSDP} (\AA^{-1})	Q_2 (\AA^{-1})	Q_3/Q_2	Q_4/Q_2	$S_{NN}(Q_2)$	$S_{NN}(Q_{\text{FSDP}})/$ $S_{NN}(Q_2)$	$S_{NN}(Q_3)/$ $S_{NN}(Q_2)$	$S_{NN}(Q_4)/$ $S_{NN}(Q_2)$
Se	–	–	–	1.92(2)	1.88	2.96	1.194(1)	–	1.176	1.015
GeSe_4	1.12(2)	0.456(5)	0.44(1)	2.04(2)	1.75	2.81	1.323(2)	0.413	1.161	0.909
GeSe_3	1.04(2)	0.598(5)	0.34(1)	2.03(2)	1.75	2.81	1.357(1)	0.491	1.159	0.881
GeSe_2	0.99(2)	0.796(5)	0.30(1)	2.02(2)	1.74	2.80	1.417(1)	0.626	1.149	0.833
$\text{GeSe}_{1.5}$	0.94(2)	0.627(5)	0.29(1)	2.02(2)	1.78	2.80	1.327(1)	0.547	1.238	0.905

Table 3. Interatomic distances and coordination numbers for glassy $\text{Ge}_x\text{Se}_{1-x}$ where r_1 and r_2 give the positions of the first and second peaks in $g_{\text{NN}}(r)$

Glass	$r_1(\text{\AA})$	r_2/r_1	\bar{n}	\bar{n} ('8-N' rule)
Se	2.34(2)	1.573	2.03(5)	2
GeSe_4	2.35(2)	1.583	2.44(6)	2.4
GeSe_3	2.35(2)	1.609	2.51(5)	2.5
GeSe_2	2.35(2)	1.647	2.69(5)	2.67
$\text{GeSe}_{1.5}$	2.37(2)	1.616	2.81(5)	2.8

believed to consist mainly of chains with perhaps a few rings.⁽¹⁹⁾

When 20 mol% Ge is added to form GeSe_4 it is anticipated to break-up and cross link the Se chain structure by forming fourfold coordinated units on the basis of the '8-N' rule. The small shift of the first peak position in $g_{\text{NN}}(r)$ to 2.35(2) Å is then consistent with the formation of $\text{Ge}(\text{Se}_{1/2})_4$ tetrahedra having a Ge–Se bonding distance of ≈ 2.36 Å, as found from the measured $g_{\text{GeSe}}(r)$ for glassy GeSe_2 .⁽²⁰⁾ An increase of the first peak position could also be compatible with the formation of homopolar Ge–Ge bonds that appear at ≈ 2.42 Å in $\text{Ge}_x\text{Se}_{1-x}$ glasses.⁽²⁰⁾ Indeed, it is not possible to unambiguously distinguish between two contrasting models for the structure of $\text{Ge}_x\text{Se}_{1-x}$ networks on the basis of the first peak of $g_{\text{NN}}(r)$ which is the function measured in conventional neutron, x-ray and electron diffraction experiments on Ge–Se glasses. In the random covalent network (RCN) model the distribution of bond types is purely statistical^(19,34) giving $\bar{n}_{\text{Ge}}^{\text{Ge}} = 8x/(1+x)$, $\bar{n}_{\text{Se}}^{\text{Se}} = 2(1-x)/(1+x)$ and $\bar{n}_{\text{Ge}}^{\text{Se}} = 4(1-x)/(1+x)$. On the other hand, in the chemically ordered network (CON) model Ge–Se bonds are favoured such that only

Ge–Se and Se–Se bonds are allowed on the Se rich side of the GeSe_2 composition ($x < 1/3$) while only Ge–Se and Ge–Ge bonds are allowed on the Ge rich side ($x > 1/3$).^(19,35) At the stoichiometric composition $x = 1/3$ only Ge–Se bonds are allowed and the network is completely chemically ordered. The expected coordination numbers for the CON are $\bar{n}_{\text{Ge}}^{\text{Se}} = 4$, $\bar{n}_{\text{Se}}^{\text{Se}} = 2(1-3x)/(1-x)$ and $\bar{n}_{\text{Ge}}^{\text{Ge}} = 0$ on the Se rich side or $\bar{n}_{\text{Ge}}^{\text{Se}} = 2(1-x)/x$, $\bar{n}_{\text{Se}}^{\text{Se}} = 0$ and $\bar{n}_{\text{Ge}}^{\text{Ge}} = 2(3x-1)/x$ on the Ge rich side. However, both the RCN and CON models give the same mean coordination number of $\bar{n} = 2(1+x)$, i.e. this \bar{n} value is simply a condition that must hold if, in accordance with the '8-N' rule, Ge is fourfold coordinated and Se is twofold coordinated in $\text{Ge}_x\text{Se}_{1-x}$ glasses.

Recent neutron diffraction experiments on glassy GeSe_2 ⁽²⁰⁾ using the method of isotopic substitution show that the chemical order of the network is broken with a maximum of 25(5)% Ge and 20(5)% Se being involved in homopolar bonds. However, the ratio of the number of Ge–Ge (or Se–Se) bonds to the total number of bonds in the glass is small at $\approx 4\%$. Further, the basic building block of the glass is the $\text{Ge}(\text{Se}_{1/2})_4$ tetrahedral unit. The analysis of the neutron diffraction results for the $\text{Ge}_x\text{Se}_{1-x}$ glasses will therefore proceed on the basis that heteropolar bonding is preferred, a strategy that is in keeping with most previous investigations.^(5,9,10,13–18)

For glassy GeSe_4 the first peak in $g_{\text{NN}}(r)$ gives a coordination number $\bar{n} = 2.44(6)$ and is consistent with the CON model wherein $\bar{n}_{\text{Ge}}^{\text{Se}} = 4$, $\bar{n}_{\text{Se}}^{\text{Se}} = 1$ and $\bar{n} = 2.4$. A higher value $\bar{n} = 2.64(18)$ was measured in a previous neutron diffraction experiment⁽⁹⁾ corresponding to $\bar{n}_{\text{Ge}}^{\text{Se}} = 4$ and

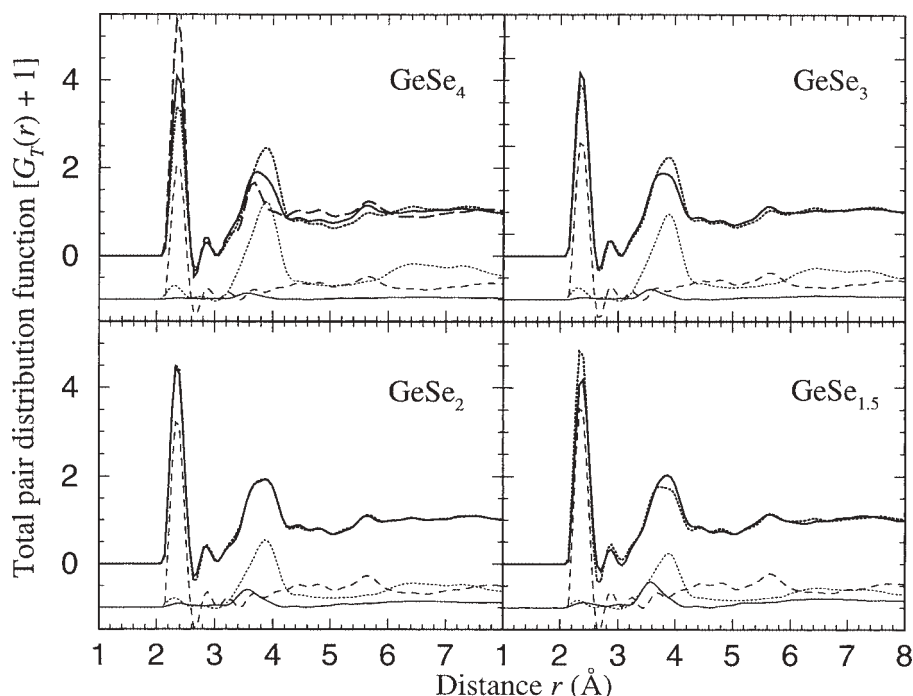


Figure 3. The measured $[G_T(r)+1] \approx g_{\text{NN}}(r)$ functions for $\text{Ge}_x\text{Se}_{1-x}$ glasses (thick solid curves) compared with the same functions constructed (thick dotted curves) by using Equation (4) to weight the Ge–Ge (solid curves), Ge–Se (dashed curves) and Se–Se (dotted curves) partial pair distribution functions measured for glassy GeSe_2 .⁽²⁰⁾ The weighted contributions of the $g_{\alpha\beta}(r)$ to $[G_T(r)+1]$ are shifted down by unity for clarity of presentation. The $[G_T(r)+1]$ function for glassy GeSe_4 was also constructed using the Se–Se pair distribution function measured for pure glassy Se (see Figure 2) in place of that measured for glassy GeSe_2 (thick long dashed curve). All of the real space functions were obtained after truncating the corresponding reciprocal space functions at the same maximum value $Q_{\text{max}} = 15.95 \text{\AA}^{-1}$

$\bar{n}_{\text{Ge}}^{\text{Se}} = 1.3(2)$ while coordination numbers of $\bar{n}_{\text{Ge}}^{\text{Ge}} = 4.1(2)$, $\bar{n}_{\text{Se}}^{\text{Se}} = 0.7(2)$ and $\bar{n} = 2.20(17)$ have been obtained from EXAFS experiments.⁽¹⁴⁾ In a recent first principles molecular dynamics simulation of liquid GeSe_4 ⁽³⁶⁾ evidence for a small number of homopolar Ge–Ge bonds was found with $\bar{n}_{\text{Ge}}^{\text{Ge}} = 3.87$, $\bar{n}_{\text{Se}}^{\text{Se}} = 1.04$, $\bar{n}_{\text{Ge}}^{\text{Ge}} = 0.06$ and $\bar{n} = 2.39$. Overall, the simulation results were, however, found to be consistent with a CON as opposed to a RCN model.

As the full set of $g_{\alpha\beta}(r)$ for glassy GeSe_2 have been measured⁽²⁰⁾ and the fundamental building block in this glass, the $\text{Ge}(\text{Se}_{1/2})_4$ tetrahedron, is also present in GeSe_4 , the $g_{\alpha\beta}(r)$ for GeSe_2 were used to construct $G_T(r) \approx [g_{\text{NN}}(r) - 1]$ for GeSe_4 by applying suitable weighting factors, Equation (4). Additionally, $G_T(r)$ was constructed by using the measured $g_{\text{SeSe}}(r)$ for glassy Se (Figure 2) in place of that for glassy GeSe_2 . For the purpose of these comparisons the r space functions were all derived by truncating the corresponding reciprocal space functions at the *same* maximum value $Q_{\text{max}} = 15.95 \text{ \AA}^{-1}$. The results shown in Figure 3 demonstrate that, while neither of these combinations reproduce $G_T(r)$ for GeSe_4 , the correlations contributing to the main features in $G_T(r)$ can be identified.

On the addition of Ge to form glassy GeSe_3 , \bar{n} increases to 2.51(5) and the ratio of the first and second peak positions, r_2/r_1 , increases to 1.609 which is closer to the ratio $r_{\text{SeSe}}/r_{\text{GeSe}} = \sqrt{8/3} = 1.633$ expected for perfect $\text{Ge}(\text{Se}_{1/2})_4$ tetrahedra. Figure 3 shows that by using the weighted $g_{\alpha\beta}(r)$ for GeSe_2 better agreement with $G_T(r)$ is obtained for GeSe_3 compared with GeSe_4 . As $\text{Ge}(\text{Se}_{1/2})_4$ motifs are formed with increasing x the first peak of $G_T(r)$ is better represented by $g_{\text{GeSe}}(r)$ for glassy GeSe_2 and the second peak position moves to higher r as it gains an increased contribution from Se–Se correlations within tetrahedra. The CON model gives coordination numbers of $\bar{n}_{\text{Ge}}^{\text{Ge}} = 4$, $\bar{n}_{\text{Se}}^{\text{Se}} = 2/3$ and $\bar{n} = 2.5$ which compare with values of $\bar{n}_{\text{Ge}}^{\text{Ge}} = 4.1(2)$, $\bar{n}_{\text{Se}}^{\text{Se}} = 0.4(2)$ and $\bar{n} = 2.35(17)$ obtained from EXAFS experiments⁽¹⁴⁾ and $\bar{n}_{\text{Ge}}^{\text{Ge}} = 3.95$, $\bar{n}_{\text{Se}}^{\text{Se}} = 0.75$ and $\bar{n} = 2.54$ obtained from a differential anomalous x-ray scattering study.⁽³⁷⁾ Overall, the diffraction results are consistent with several Raman spectroscopy studies of $\text{Ge}_x\text{Se}_{1-x}$ glasses where both $(\text{Se})_n$ chains and $\text{Ge}(\text{Se}_{1/2})_4$ tetrahedra are found at small x values.^(3,5,17,18)

For GeSe_2 , the comparison of Figure 3 confirms that the $G_T(r)$ function measured using the SANDALS time of flight instrument can be adequately represented by the weighted $g_{\alpha\beta}(r)$ measured using the D4B reactor-source diffractometer.⁽²⁰⁾ The $g_{\alpha\beta}(r)$ give a ratio $r_{\text{SeSe}}/r_{\text{GeSe}} = 1.647$, close to the value expected for perfect tetrahedral coordination of Ge, and show that 34(5)% of the Ge are involved in edge sharing tetrahedra, in accordance with other estimates. For example, the fraction of Ge involved in edge sharing tetrahedra has been estimated at 33% by an analysis of Raman spectroscopy data.⁽³⁸⁾ and at 40% by an analysis of $G_T(r)$ as measured using neutron diffraction.⁽³⁹⁾ Nearest neighbour coordination numbers of $\bar{n}_{\text{Ge}}^{\text{Se}} = 3.7(1)$, $\bar{n}_{\text{Se}}^{\text{Se}} = 0.20(5)$ and $\bar{n}_{\text{Ge}}^{\text{Ge}} = 0.25(5)$ were obtained which corresponds to $\bar{n} = 2.68(6)$ and compares with $\bar{n} = 2.69(5)$ obtained in the present work. Further evidence for broken chemi-

cal ordering in liquid and glassy GeSe_2 comes from other studies using neutron diffraction,⁽⁴⁰⁾ spectroscopy^(16,38,41–45) and molecular dynamics simulation.^(46–50)

For glassy $\text{GeSe}_{1.5}$ the first peak in $g_{\text{NN}}(r)$ occurs at a higher r value than for the other compositions. This can be understood in terms of the disappearance of Ge–Se and Se–Se bonds at $\approx 2.36 \text{ \AA}$ and $\approx 2.32 \text{ \AA}$, respectively, and the appearance of additional homopolar Ge–Ge bonds at $\approx 2.42 \text{ \AA}$.⁽²⁰⁾ The first peak in $g_{\text{NN}}(r)$ gives $\bar{n} = 2.81(5)$ which is consistent with the CON model for which $\bar{n}_{\text{Ge}}^{\text{Se}} = 3$, $\bar{n}_{\text{Ge}}^{\text{Ge}} = 1$, $\bar{n}_{\text{Se}}^{\text{Se}} = 0$ and $\bar{n} = 2.8$. A value of $\bar{n} = 2.88(18)$ was obtained in a previous neutron diffraction experiment⁽⁹⁾ corresponding to $\bar{n}_{\text{Ge}}^{\text{Se}} = 3.1(2)$ and $\bar{n}_{\text{Ge}}^{\text{Ge}} = 1$ while coordination numbers of $\bar{n}_{\text{Ge}}^{\text{Se}} = 3.0(3)$, $\bar{n}_{\text{Ge}}^{\text{Ge}} = 1.0(2)$ and $\bar{n} = 2.80(19)$ were found from EXAFS experiments.⁽¹⁴⁾ The results are consistent with the presence of $\text{Ge}_2\text{Se}_{6/2}$ ethane like units in glassy $\text{GeSe}_{1.5}$, a model that has been proposed on the basis of several spectroscopic studies.^(16,38,41,45,51)

By comparison with the measured partial structure factors for liquid and glassy GeSe_2 ^(20,40) the FSDP in $S_{\text{NN}}(Q)$ for the $\text{Ge}_x\text{Se}_{1-x}$ glasses will arise predominantly from Ge–Ge correlations. This assignment is fully consistent with differential anomalous x-ray scattering studies made on $\text{Ge}_x\text{Se}_{1-x}$ glasses.^(37,52,53) With increasing x the periodicity, $2\pi/Q_{\text{FSDP}}$, of the associated intermediate ranged oscillations increases from 5.6 to 6.7 \AA and their coherence length, $2\pi/\Delta Q_{\text{FSDP}}$, increases from 14.2 to 21.7 \AA . This trend for $\text{Ge}_x\text{Se}_{1-x}$ glasses is confirmed by other diffraction experiments.^(9,11) The height of the FSDP reaches its maximum at the $x = 1/3$ composition in both the glassy (Table 1) and liquid^(6,7) phases of $\text{Ge}_x\text{Se}_{1-x}$ where the molar volume also shows a maximum^(54,55) and where the optimum number of $\text{Ge}(\text{Se}_{1/2})_4$ tetrahedra is expected on the basis of the CON model. The associated intermediate ranged oscillations in r space have, therefore, their largest amplitude at the GeSe_2 composition and are actually discernible in the measured $g_{\text{GeGe}}(r)$.⁽²⁴⁾ For the liquid state of GeSe , the FSDP is a weak feature in $S_{\text{NN}}(Q)$ but is not manifested in any of the so-called Faber–Ziman partial structure factors.⁽⁵⁶⁾

Conclusions

The structure of the $\text{Ge}_x\text{Se}_{1-x}$ ($0 \leq x \leq 0.4$) glasses was analysed by reference to the measured full set of partial pair distribution functions for glassy GeSe_2 .⁽²⁰⁾ As manifested by the appearance of a first sharp diffraction peak at $\approx 1 \text{ \AA}^{-1}$, the addition of Ge to glassy Se invokes an additional length scale in the atomic ordering that is associated with intermediate ranged Ge–Ge correlations. The results are consistent with the ‘8-N’ rule and may be interpreted in terms of a chemically ordered continuous random network model. However, the full set of $g_{\alpha\beta}(r)$ measured for glassy GeSe_2 show that deviations from this model do occur and may, therefore, be expected for other glasses near this composition.

Acknowledgements

Chris Benmore (ISIS), Henry Fischer (ILL) and Pierre Palleau (ILL) are thanked for their help with the experiments. I. Petri thanks the University of East Anglia for financial support.

References

- Bhatia, A. B. & Thornton, D. E. *Phys. Rev. B*, 1970, **2**, 3004.
- Azoulay, R., Thibierge, H. & Brenac, A. *J. Non-Cryst. Solids*, 1975, **18**, 33.
- Feng, X., Bresser, W. J. & Boolchand, P. *Phys. Rev. Lett.*, 1997, **78**, 4422.
- Boolchand, P., Bresser, W. J., Georgiev, D. G., Wang, Y. & Wells, J. In *Phase transitions and self-organization in electronic and molecular networks*. 2001. Edited by J. C. Phillips & M. F. Thorpe. Kluwer Academic, Dordrecht. P 65.
- Wang, Y., Matsuda, O., Inoue, K., Yamamuro, O., Matsuo, T. & Murase, K. *J. Non-Cryst. Solids*, 1998, **232-234**, 702.
- Salmon, P. S. & Liu, J. *J. Phys.: Condens. Matter*, 1994, **6**, 1449.
- Maruyama, K., Misawa, M., Inui, M., Takeda, S., Kawakita, Y. & Tamaki, S. *J. Non-Cryst. Solids*, 1996, **205-207**, 106.
- Petri, I., Salmon, P. S. & Howells, W. S. *J. Phys.: Condens. Matter*, 1999, **11**, 10219.
- Ramesh Rao, N., Krishna, P. S. R., Basu, S., Dasannacharya, B. A., Sangunni, K. S. & Gopal, E. S. R. *J. Non-Cryst. Solids*, 1998, **240**, 221.
- Malaurent, J. C. & Dixmier, J. *J. Non-Cryst. Solids*, 1980, **35-36**, 1227.
- Hafiz, M. M., Hammad, F. H. & El-Kabany, N. A. *Physica B*, 1993, **183**, 392.
- Fawcett, R. W., Wagner, C. N. J. & Cargill, G. S. *J. Non-Cryst. Solids*, 1972, **8-10**, 369.
- Uemura, O., Sagara, Y. & Satow, T. *Phys. Status Solidi A*, 1974, **26**, 99.
- Zhou, W., Paesler, M. & Sayers, D. E. *Phys. Rev. B*, 1991, **43**, 2315.
- Gulbrandsen, E., Johnsen, H. B., Endregaard, M., Grande, T. & Stølen, S. *J. Solid State Chem.*, 1999, **145**, 253.
- Mamedov, S. B., Aksenov, N. D., Makarov, L. L. & Batrakov, Yu. F. *J. Non-Cryst. Solids*, 1996, **195**, 272.
- Tronc, P., Bensoussan, M., Brenac, A. & Sebenne, C. *Phys. Rev. B*, 1973, **8**, 5947.
- Sugai, S. *Phys. Rev. B*, 1987, **35**, 1345.
- Elliott, S. R. *Physics of Amorphous Materials*. 2nd Edition. 1990. Longman, Harlow.
- Petri, I., Salmon, P. S. & Fischer, H. E. *Phys. Rev. Lett.*, 2000, **84**, 2413.
- Wright, A. C., Sinclair, R. N. & Leadbetter, A. J. *J. Non-Cryst. Solids*, 1985, **71**, 295.
- Salmon, P. S. *Proc. R. Soc. Lond. A*, 1992, **437**, 591.
- Price, D. L., Moss, S. C., Reijers, R., Saboungi, M. -L. & Susman, S. *J. Phys. C: Solid State Phys.*, 1988, **21**, L1069.
- Salmon, P. S. *Proc. R. Soc. Lond. A*, 1994, **445**, 351.
- Sears, V. F. *Neutron News*, 1992, **3**, 26.
- Borisova, Z. U. *Glassy Semiconductors*. 1981. Plenum, New York.
- Feltz, A. & Lippmann, F. J. *Z. Anorg. Allg. Chem.*, 1973, **398**, 157.
- Sarrach, D. J., De Neufville, J. P. & Haworth, W. L. *J. Non-Cryst. Solids*, 1976, **22**, 245.
- Wagner, T., Kasap, S. O. & Maeda, K. *J. Mater. Res.*, 1997, **12**, 1892.
- Bertagnoli, H., Chieux, P. & Zeidler, M. D. *Molec. Phys.*, 1976, **32**, 759.
- Soper, A. K., Howells, W. S. & Hannon, A. C. *Rutherford Appleton Laboratory Report*. 1989. RAL-89-046.
- Salmon, P. S. *J. Phys. F: Met. Phys.*, 1988, **18**, 2345.
- Salmon, P. S. & Benmore, C. J. In *Recent developments in the physics of fluids*. 1992. Edited by W. S. Howells & A. K. Soper. Adam Hilger, Bristol. P F225.
- Liang, K. S., Bienenstock, A. & Bates, C. W. *Phys. Rev. B*, 1974, **10**, 1528.
- White, R. M. *J. Non-Cryst. Solids*, 1974, **16**, 387.
- Haye, M. J., Massobrio, C., Pasquarello, A., De Vita, A., De Leeuw, S. W. & Car, R. *Phys. Rev. B*, 1988, **58**, R14661.
- Armand, P., Ibanez, A., Ma, Q., Raoux, D. & Philippot, E. *J. Non-Cryst. Solids*, 1993, **167**, 37.
- Jackson, K., Briley, A., Grossman, S., Porezag, D. V. & Pederson, M. R. *Phys. Rev. B*, 1999, **60**, R14985.
- Susman, S., Volin, K. J., Montague, D. G. & Price, D. L. *J. Non-Cryst. Solids*, 1990, **125**, 168.
- Penfold, I. T. & Salmon, P. S. *Phys. Rev. Lett.*, 1991, **67**, 97.
- Nemanich, R. J., Connell, G. A. N., Hayes, T. M. & Street, R. A. *Phys. Rev. B*, 1978, **18**, 6900.
- Bridenbaugh, P. M., Espinosa, G. P., Griffiths, J. E., Phillips, J. C. & Remeika, J. P. *Phys. Rev. B*, 1979, **20**, 4140.
- Bresser, W. J., Boolchand, P., Suranyi, P. and de Neufville, J. P. *Phys. Rev. Lett.*, 1981, **46**, 1689.
- Boolchand, P., Grothaus, J., Bresser, W. J. & Suranyi, P. *Phys. Rev. B*, 1982, **25**, 2975.
- Boolchand, P. & Bresser, W. J. *Phil. Mag. B*, 2000, **80**, 1757.
- Cobb, M., Drabold, D. A. & Cappelletti, R. L. *Phys. Rev. B*, 1996, **54**, 12162.
- Cobb, M. & Drabold, D. A. *Phys. Rev. B*, 1997, **56**, 3054.
- Massobrio, C., Pasquarello, A. & Car, R. *Phys. Rev. Lett.*, 1998, **80**, 2342.
- Massobrio, C., Pasquarello, A. & Car, R. *J. Am. Chem. Soc.*, 1999, **121**, 2943.
- Zhang, X. & Drabold, D. A. *Phys. Rev. B*, 2000, **62**, 15695.
- Lucovsky, G., Nemanich, R. J. & Galeener, F. L. In *Proc. Seventh Int. Conf. on Amorphous and Liquid Semiconductors*. 1977. Edited by W. E. Spear. University of Edinburgh, Edinburgh. P 130.
- Fuoss, P. H., Eisenberger, P., Warburton, W. K. & Bienenstock, A. *Phys. Rev. Lett.*, 1981, **46**, 1537.
- Fischer-Colbrie, A. & Fuoss, P. H. *J. Non-Cryst. Solids*, 1990, **126**, 1.
- Feltz, A. *Amorphous inorganic materials and glasses*. 1993. VCH, Weinheim.
- Ruska, J. & Thurn, H. *J. Non-Cryst. Solids*, 1976, **22**, 277.
- Petri, I., Salmon, P. S. & Fischer, H. E. *J. Phys.: Condens. Matter*, 1999, **11**, 7051.